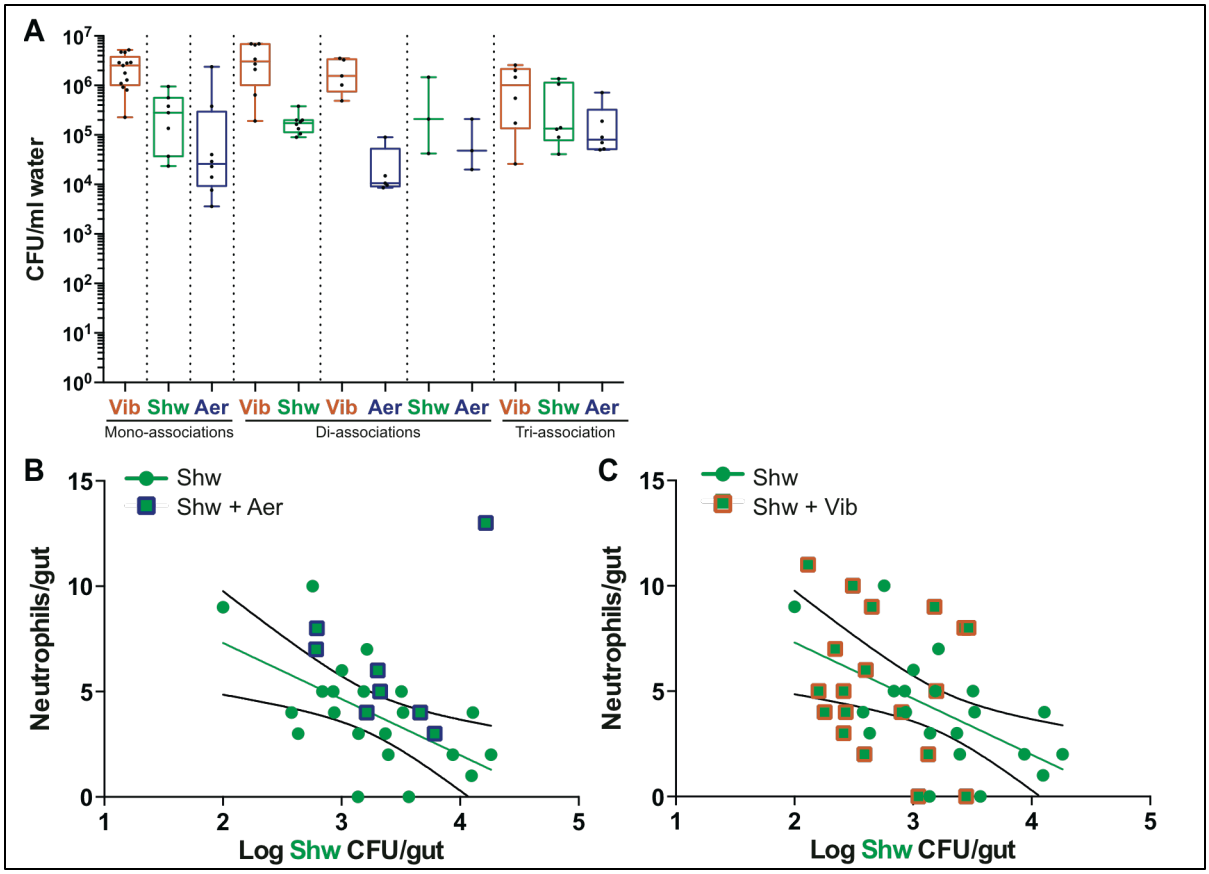

Figure S1. Microbial di-associations reveal complex dynamics between microbes.

(Related to Figure 2) (A) Each species was inoculated into the fish media at 10^6 CFU/ml at 4dpf. At 6 dpf, when the fish were examined, a sample was taken to examine the concentration of bacteria in the media at that time. Concentrations of *Vibrio* (red), *Shewanella* (green), and *Aeromonas* (blue) in the fish media (EM) are unaltered comparing the mono-associations (single columns, left), to the di-associations (double columns, middle), and the tri-association (triple columns, right). This suggests that dynamics between colonization of these species in the host are host-associated. *Shewanella* abundance in di-association with *Aeromonas* **(B)** or *Vibrio* **(C)** appears to maintain the relationship with intestinal neutrophil influx that it establishes in mono-association (green circles). The linear relationship for each di-association is not significant and is also not significantly different from the linear relationship for the mono-association. For each di-association, one representative independent experiment is shown.

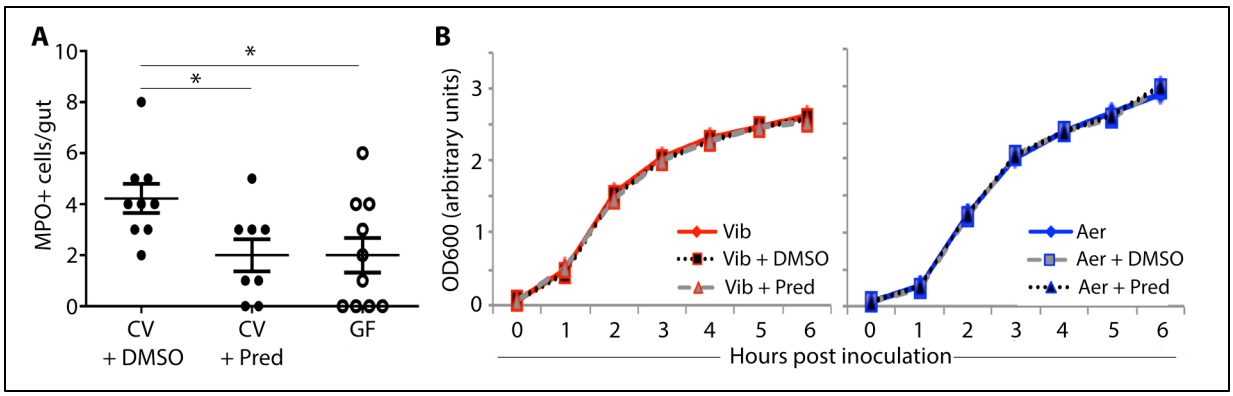

Figure S2. Prednisolone does not affect *in vitro* growth (Related to Figure 3). A. Treatment of conventionally raised (CV) zebrafish with 25 μg/mL prednisolone reduces intestinal neutrophil influx. GF, germ-free. **B.** *In vitro* growth of *Vibrio* (left panel) or *Aeromonas* (right panel) is unaffected by the presence of 25 μg/mL prednisolone. DMSO, vehicle control.

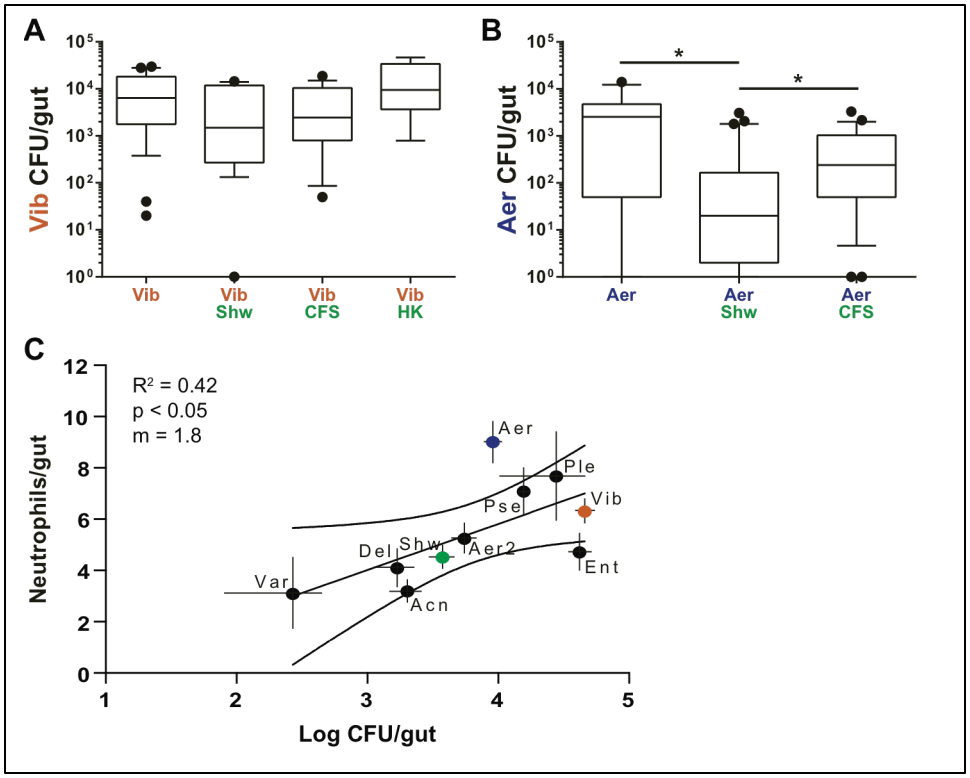

Figure S3. Effects of *Shewanella* and *Shewanella* CFS on *Vibrio* and *Aeromonas* (Related to Figure 4). A. Co-inoculating *Vibrio* with either live *Shewanella, Shewanella* cell-free supernatant (CFS), or heat-killed (HK) *Shewanella* does not change the abundance of *Vibrio* in the intestine compared to a *Vibrio* mono-association. **B.** Co-inoculating *Aeromonas* with *Shewanella* significantly reduces the abundance of *Aeromonas* compared to a mono-association. Co-inoculating *Aeromonas* with *Shewanella* CFS does not change the abundance of *Aeromonas* compared to a mono-association. *p < 0.05, Students T-test. **C.** (Related to methods: Gnotobiotic zebrafish husbandry and microbiology)**.** Linear correlation between the average number of neutrophils per intestine and the logarithm of the average colony-forming units (CFU) per intestine for all mono-associations (error bars in both directions are SEM). Dashed line indicates the 95% confidence interval for the correlation. *Aeromonas* appears to be an outlier and was included in statistical analysis. Aer, *Aeromonas sp. 1;* Vib, *Vibrio;* Ple, *Plesiomonas;* Shw, *Shewanella;* Aer2, *Aeromonas sp. 2;* Ent, *Enterobacter;* Pse, *Pseudomonas;* Del, *Delftia;* Var, *Variovorax;* Acn, *Acinetobacter.*

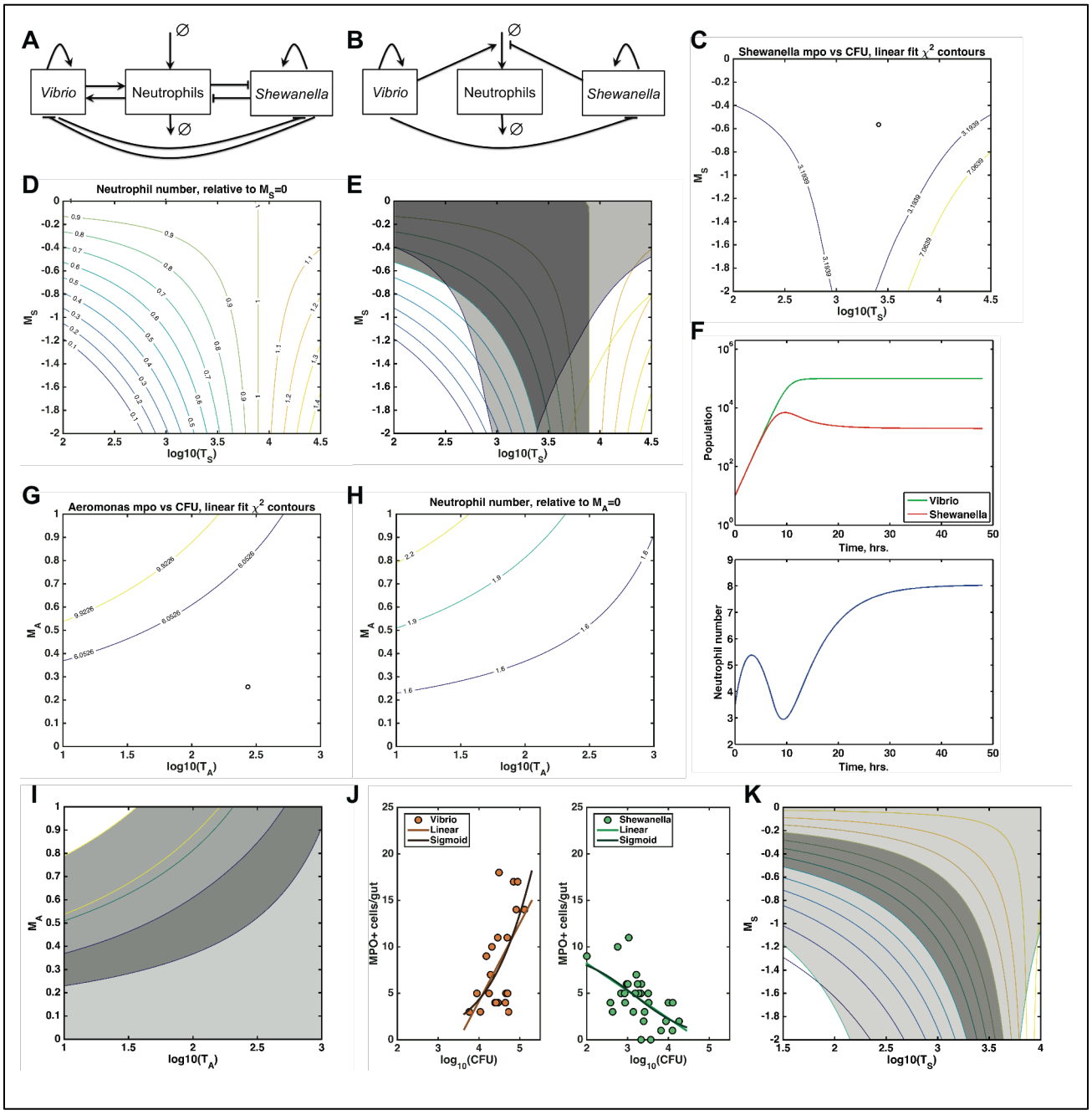

Figure S4. Modeling bacterial/neutrophil interactions (Related to Experimental procedures: Statistics and modeling). A. Schematic interaction network. Interactions can be positive (arrowheads) or negative (bars). Sources and sinks are depicted by ∅. For concreteness we have illustrated a particular set that corresponds to observations described in the main text. **B.** Simplified schematic interaction network. **C.** Goodness of fit for *Shewanella* mono-association neutrophil number (linear fit). The circle indicates the best-fit parameters. The

contours are the 68% and 95% confidence intervals. **D.** Neutrophils: predicted suppression factor ζ_{VS} for *Vibrio-Shewanella* di-association. **E.** *Shewanella* → neutrophil parameter space. The dark shaded region is that for which the parameters in the additive interaction model are consistent with both the *Shewanella* mono- and di-association data. **F.** Simulated time series with "best-fit" model parameters. The upper graph shows the bacterial populations; the lower graph shows the neutrophil number. **G.** Goodness of fit for *Aeromonas* mono-association neutrophil number (linear fit). The circle indicates the best-fit parameters. The contours are the 68% and 95% confidence intervals. **H.** Neutrophils: predicted enhancement factor, ζ_{VA}, for *Vibrio-Aeromonas* di-association. **I.** *Aeromonas* → neutrophil parameter space. The dark shaded region is that for which the parameters in the additive interaction model are consistent with both the *Aeromonas* mono- and di-association data. **J.** Neutrophil count vs. bacterial abundance (CFU), as in Figure 1, with fits to a model that is linear in log(CFU), and a model that is sigmoidal in log(CFU), for *Vibrio* (left) and *Shewanella* (right) mono-associations. **K.** *Shewanella* → neutrophil parameter space for a sigmoidal bacterial → neutrophil response function. The dark shaded region is that for which the parameters in the additive interaction model are consistent with both the *Shewanella* mono- and di-association data.

Supplemental experimental materials

Gnotobiotic zebrafish husbandry

Zebrafish embryos were derived germ free (GF) by the following procedure. Embryos 6 hours post fertilization were soaked in 0.1% polyvinylpyrrolidone-iodine (PVP-I, Sigma, St. Louis, MO) for 2 min, washed three times in sterile embryo medium (EM), soaked in 0.003% bleach for 10 minutes, then washed in sterile EM. Subsequently, 15 GF embryos were transferred to sterile tissue culture flasks (25 cm^2, Techno Plastic Products, Trasadingen, Switzerland) with 15-mL sterile EM. Sterility of GF flasks was confirmed visually using phase optics on a 40x magnification and by culturing. Control conventionalized (CVZ) fish were prepared GF, as above, and inoculated with 1 mL of non-sterile conventional embryo media (EM) on 4 dpf. Inoculating flasks containing 4 dpf GF zebrafish with 10^6 CFU/mL of each bacterial strain generated mono-, di-, or tri-associated zebrafish. All manipulations to the GF flasks were performed under a class II A/B3 biological safety cabinet. The flasks were kept at 28° C until analysis of fluorescent cells on 6 dpf. Zebrafish were anesthetized in Tricaine (Stock 4g/L, Western Chemical, Inc., Ferndale, WA). Zebrafish intestines were dissected using sterile dissecting needles. The fish was oriented with the intestinal bulb towards the right. One dissecting needle was placed above and to the left of the intestinal bulb; the second needle was placed on the fish to hold it in place. Subsequently, the needle placed by the bulb was pulled to the right, dislodging the bulb from the esophageal-intestinal junction. Then the entire intestine was pulled out of the fish. Intestines that were torn in the process were not included in colonization analysis.

Microbiology

From freezer stocks, the bacterial isolates were grown aerobically on tryptic soy agar (TSA, BD, Sparks, MD) at 30° C. For fish inoculations these strains were grown shaking,

aerobically in tryptic soy broth (TSB, BD, Sparks MD) over night at 30° C, then diluted in sterile EM before inoculation.

Prednisolone treatments

The prednisolone solution was prepared by dissolving 6α-methylprednisolone (Sigma, St. Louis, MO) in di-methyl sulfoxide (DMSO, Fisher, Fair Lawn, NJ) and filter sterilizing (DMSO-safe, Fisher Scientific, Waltham, MA). Gnotobiotic zebrafish were treated with a final concentration of 25 ug/ml. A DMSO-only vehicle control was included in all prednisolone experiments.

Microbiota quantification

To determine the CFU/intestine, dissected zebrafish intestines were placed in 100-ul sterile EM. Each gut was homogenized with a cordless pestle motor (VWR) and a sterile disposable pestle (VWR) for 30 seconds. Samples were subsequently diluted, and cultured on TSA (BD, Sparks MD). The TSA plates were incubated aerobically at 30° C overnight and then colonies were counted.

Concentration of cell-free supernatant

Shewanella was grown over night shaking in TSB. Then 1 ml of the overnight culture was used to inoculate a 50-ml culture, which was kept shaking at 30º C for 2 h. To prepare the CFS, the 50-mL cultures were centrifuged at 7000 × g for 10 min at 4º C. Subsequently, the supernatant was filtered through a 0.22-m sterile tube top filter (Corning Inc., Corning, NY). The sterile supernatant was concentrated at 4º C for 1 h at 3000 × g with a centrifugal device that has a 10-kda weight cut off (Pall Life Sciences,

Ann Arbor, MI). The concentration of the supernatant was determined with a Nanodrop and inoculated into the flasks at a final concentration of 500 ng/mL.

In vitro co-culture assay

Vibrio and *Aeromonas* were grown overnight shaking in TSB (BD, Sparks, MD). 5×10^8 bacterial cells of each strain were mixed together and brought up to a volume of 1 ml with sterile TSB. A co-culture of an isogenic fluorescently tagged strain with the wild-type counterpart served as controls. The homogenate was diluted and plated to obtain the starting ratio of the two bacterial strains. The bacterial mixture was centrifuged for 2 min at 7000 × g and re-suspended in 30 μL brain heart infusion media (BHI, BD, Sparks, MD). This re-suspension was spotted directly on sterile 0.46-μm filter paper (Millipore, Darmstadt, Germany) that had been placed directly on a BHI-agar plate. We also performed these assays on TSA plates but saw a smaller effect. Plates were incubated for 24 h at 30° C. Bacterial spots were harvested and the CFU/mL of surviving bacteria was measured by serial dilution and plating.

Modeling bacteria-neutrophil interactions

We describe a model of bacteria and neutrophil populations dynamics, motivated by the experiments described in the main text. In general, the possible interactions between two bacterial species, for example *Vibrio* and *Shewanella,* can be depicted as in Figure S4A. Interactions can be positive or negative. Our goal is a very simple, lowest-order model that parameterizes key aspects of bacterial growth, neutrophil influx, and interactions between two bacterial components and neutrophils with a minimal number of parameters, to avoid over-fitting. Moreover, the model described below helps determine whether additive interactions between species' effects are capable of

reproducing observed phenomena. Of course, more complex interactions may exist in reality, which could be uncovered in future experiments.

With *no interactions* between neutrophils and bacteria, but interactions between two bacterial species *i* and *j,* let us consider this model:

(1) $$\frac{dP_i}{dt} = r_i P_i (1 - \frac{P_i + \gamma_{ij} P_i}{K_i})$$

(2) $$\frac{dN}{dt} = \alpha_N - k_N N$$

Here, *i* and *j* label the bacterial species (e.g. *Vibrio* and *Shewanella), P_i* is the population of species *i, N* is the number of neutrophils, and the other symbols are defined below. All the P_i, as well as *N,* are constrained to be non-negative. The first equation represents Lotka-Volterra dynamics for two interactions species, while the second is a linear model of neutrophil flux. There are several parameters: r_i, the growth rate of species *i;* K_i, the carrying capacity of species *i;* γ_{ij}, parameters characterizing interactions, specifically the influence of species *j* on species *i;* α_N, the influx rate of neutrophils; k_N, the exit rate of neutrophils. At steady state, the number of neutrophils is clearly $N = \alpha_N / k_N$.

Now let's introduce *interactions* between neutrophils and bacteria. Bacterial might influence the influx (or exit) of neutrophils, and neutrophils might influence bacterial growth rates. The latter could be represented by:

(3) $$\frac{dP_i}{dt} = r_i P_i \left(1 - \frac{P_i + \gamma_{ij} P_j - b_i N}{K_i}\right)$$

Introducing new parameters b_i. Considering terms like this, we find reasonable agreement with the data only for $b \approx 0$ (not shown). Moreover, since we are looking to see whether a minimal model is sufficient to describe the data, will ignore these neutrophil → bacteria interactions. Let us consider bacteria → neutrophil interactions by replacing equation 2 with:

(4) $$\frac{dN}{dt} = \alpha_N - k_N N + \sum_i \alpha_i(P_i)$$

Where $\alpha_i(P_i)$ characterizes the effect of species *i* on neutrophil influx. The influence of bacteria on neutrophils is given by an influx-like term. Importantly, in this model, the two extra influx terms are simply additive. We choose the form of the influx functions to be linear in the logarithm of bacterial populations, mimicking the observations of bacterial mono-association data (Fig. 1). We will discuss a model in which the neutrophil response is a sigmoidal function of the logarithm of the population, which leads to very similar conclusions.

For *Vibrio* (V), *Shewanella* (S), and *Aeromonas* (A), we have equations 5, 6, and 7:

$$\alpha_V(P_V) = \begin{cases} M_V \log_{10} \frac{P_V}{T_V} \text{ if } P_V > T_V \\ 0 \text{ otherwise} \end{cases}$$

$$\alpha_S(P_S) = M_S \log_{10} \frac{P_S}{T_S}$$

$$\alpha_A(P_A) = M_A \log_{10} \frac{P_A}{T_A}$$

For *Vibrio*, the data do not suggest any accessible regime with suppression of neutrophil number—the slope is steep and the neutrophil counts are almost always above the germ-free value, ≈ 3.5 (Fig. 1). Therefore, T_V is a sharp population threshold for the species' influence on neutrophils. For *Shewanella*, $\alpha_S(P_S)$can be positive or negative, depending on whether the population is above or below T_S; the data imply that the neutrophil interaction can be positive or negative, since the neutrophil counts lie above and below the germ-free value . Of course, the above form must fail to describe the system for low P_S, since it does not approach the germ-free neutrophil abundance as $P_S \to 0$. We would expect the slopes M_V, M_S, and M_A to be positive, negative, and near

zero, respectively, given the data; this will be assessed more rigorously below.

Equations 1 and 4-7 define our model. Some of its properties can be assessed simply by inspection. For others we numerically integrate these differential equations, starting from initial populations P_i = 10 bacteria and N = 3.5 neutrophils, over a span of 48 hours using programs written in MATLAB that make use of MATLAB's ``ode45'' numerical integration function. In all cases, the system reaches a steady state within this interval.

Incorporating interactions has added new parameters to the model: M_i, magnitude of the influence of species i on the influx rate of neutrophils; T_i, characteristic population (or threshold) for the influence of species i on the influx rate of neutrophils. In total, the model has 12 parameters for two species. Some of these parameters are "uninteresting"—the growth rates (r) and carrying capacities (K), for example, which set overall timescales and population scales. The neutrophil parameters α_N and k_N only influence the background level of neutrophils by their ratio. Also, given the observed data, we can state $\gamma_{VS} \approx 0$ (i.e. the influence of *Shewanella* on *Vibrio* growth is negligible); similarly, $\gamma_{VA} \approx 0$. All this leaves us with only five "interesting" parameters for a *Vibrio*-*Shewanella* di-association: γ_{SV}, M_V, M_S, T_V, and T_S; there is a similar set for *Vibrio*-*Aeromonas* (Fig. S4B).

Growth rates for the various bacterial species in the larval zebrafish gut are known experimentally. For each (*Vibrio*, *Aeromonas*, and *Shewanella*), $r \approx 0.9$/hr. From mono-association data, the maximum number of bacteria observed provides an estimate of the carrying capacities: $K_V \approx 1 \times 10^5$, $K_S \approx 1 \times 10^{4.2}$, $K_A \approx 1 \times 10^{4.6}$. The mean number of neutrophils in germ-free fish ≈ 3.5, sets $\alpha_N / k_N = 3.5$. In simulations, we arbitrarily set $\alpha_N = 0.7$ 1/hr, $k_N = 0.2$ 1/hr; note that only the ratio matters in the steady state.

We can use the *Vibrio* mono-association data (Fig. 1D) to determine reasonable values for M_V and T_V. Given the experiment duration, growth rates, and carrying

capacity, the bacterial population will reach carrying capacity well before the experimental count of neutrophil number is made (i.e. we will observe the steady-state neutrophil number). Since $dN/dt = 0$, it follows from Eq. 4-5 that N is a simple linear function of $\log(P_V)$ for $P_V > T_V$:

(8) $$N = \frac{1}{k_N}\left(\alpha_N + M_V(\log_{10}(P_V / T_V)\right)$$

This form is consistent with the mono-association data (Fig. 1D), which we can fit with a simple linear regression to determine the parameters. (We fit N vs. log(CFU) with a simple least-squares minimization, i.e. assuming Gaussian noise; the data don't support anything more complicated.) This gives $M_V = 1.7 \pm 0.6$ 1/hr, and a threshold value of $T_V = 3.9 \pm 0.2$. We can use the bacterial population data from the *Vibrio* and *Shewanella* di-association to set γ_{SV}. Noting that with *Vibrio* present, the *Shewanella* population is reduced by a factor of 0.2 relative to *Shewanella* mono-association, we can simulate Equations 1 and 4-7, varying K_V and fixing $K_S = 0.1K_V$, for various γ_{SV} to determine the value at which P_S is reduced by 0.2× relative to $\gamma_{SV} = 0$. This gives $\gamma_{SV} \approx 0.08 \pm 0.01$. In principle, we could use the same approach as with the *Vibrio* mono-association data to extract M_S and T_S from the *Shewanella* mono-association data. Then, with all parameters fixed, we could simulate the di-association experiments and examine the predicted neutrophil abundance. However, the data are too noisy to do this with high confidence. We can see this by plotting the goodness of fit (χ^2) contours for Equation 6 applied to the *Shewanella* mono-association data as a function of M_S and T_S (Fig. S4C). The range over which χ^2 goes to +2.3 from its minimal value, i.e. the 68% confidence interval, is large. We instead take a different approach, examining ranges of M_S and T_S, simulating the resulting di-association behavior, and comparing to experimental observations. We denote as ζ_{VS} the factor by which the neutrophil number in the *Vibrio*-

Shewanella di-associations differs from the neutrophil number for *Vibrio* mono-associations. Figure S4D shows ζ_{VS} as a function of M_S and T_S, calculated from the simulations as the number of neutrophils at 48 h divided by the value for $M_S = 0$. Note that these predicted neutrophil abundances do not account for uncertainties in the parameters M_V, T_V, etc., and so the contours are actually "fuzzier" than shown. Experimentally, $\zeta_{VS} \approx 0.8 \pm 0.2$ (Fig. 4B). Does the region of the parameter space for which the model would give $\zeta_{VS} \approx 0.8 \pm 0.2$ (Fig. S4D) intersect the (large) confidence interval inferred from the mono-association data (Fig. 4)? Yes (Fig. S4E). We can therefore conclude that this simple additive model of bacteria-neutrophil interactions is consistent with the observed data. With parameters $M_V = 1.2$ 1/hr, $T_V = 3.9$, $\gamma_{SV} = 0.08$, $M_S = -0.75$, and $T_S = 2.75$, i.e. well inside the confidence interval for these parameters, the time-series implied by the model are shown in Figure S4F. It is interesting to note the non-monotonicity of the neutrophil response, which follows from the different effective thresholds of the two species' effects on neutrophil dynamics.

We can similarly examine the *Vibrio-Aeromonas* di-association data. As we would expect from the mono-association data (Fig. 1), the slope parameter M_A is moderately well constrained, but T_A is not. Again, we can consider the confidence interval (Fig. S4G). The 68% confidence interval is quite large; the threshold T_A is not at all well constrained, since the slope M_A is quite flat. Note also that behavior at low bacterial abundance is not properly accounted for in this model: at low P_A, the neutrophil number should drop to the germ-free level, which is not accounted for in the fit, and which would push M_A to a tighter band around 0.4. Examining the $\approx 10\times$ suppression of the *Aeromonas* population by *Vibrio* and the $\approx 3\times$ enhancement of the *Vibrio* population in di-associations relative to its mono-association value lets us set the interaction terms $\gamma_{AV} \approx 0.08$ and $\gamma_{VA} \approx -50$. The observed number of neutrophils for the *Vibrio-Aeromonas*

di-association is about twice that of the *Vibrio* mono-association (11.8 ± 5.2 vs. 6.2 ± 4.8), so $\xi_{VA} \approx 1.9 \pm 0.3$. The ξ_{VA} predicted by the model as a function of M_A and T_A are shown in Figure S4H. Again, χ^2 contours do not account for the large uncertainties in γ_{AV} and other parameters, and so should be considered "fuzzier" than they appear. As with the *Shewanella* parameters, we can consider the M_A / T_A parameter space for regions that would fit both the mono-association and di-association data (Fig. S4I). Again, there is considerable overlap, indicating that this simple additive model of bacteria-neutrophil interactions is sufficient to describe the *Aeromonas*-*Vibrio* data as well as the *Shewanella*-*Vibrio* data.

As noted, we model the influence of bacteria on neutrophil number with a logarithmic relationship, i.e. treating the neutrophil influx as a linear function of the logarithm of the bacterial abundance. In reality, the neutrophil population is of course bounded from above, which would motivate using a bounded fitting function such as a sigmoidal curve. However, the data do not span a range that shows the saturation of neutrophil number with increasing bacterial population, so fitting a sigmoid leaves the saturation parameter highly unconstrained. A sigmoidal fit therefore introduces an unwarranted extra degree of freedom. Nonetheless, to see if it alters any of our conclusions, we have fit the neutrophil (MPX+) vs. bacteria (CFU) data to a sigmoid. In brief, it does not. We can compare the original model, equations 9 and 10, (in which MPX+ number varies linearly with log(CFU)):

$$\alpha_i(P_i) = M_i \log_{10} \frac{P_i}{T_i}$$

$$N = \frac{1}{k_N}(\alpha_N + \alpha_i(P_i))$$

with a sigmoidal model (equations 11 and 12):

$$\alpha_i(P_i) = -\alpha_N + \frac{S_i}{1+\exp(-M_i \log_{10}\frac{P_i}{T_i})}$$

$$N = \frac{1}{k_N}(\alpha_N + \alpha_i(P_i))$$

The sigmoidal model adds a new parameter, the saturation value S_i, and it is constructed such that its limits are 0 and S_i. The parameters M_i and T_i have the same physical interpretations as in the earlier model: M_i describes steepness of the curve, and T_i is like a population offset. We illustrate the results of fits to each model (linear-logarithmic and sigmoidal-logarithmic) for *Vibrio* and *Shewanella* mono-association data (Fig. S4J). Unsurprisingly, the both models perform similarly in fitting the data, and the uncertainty in the S_i parameter is enormous (over 100% for the *Vibrio* dataset, and about 50% for *Shewanella*). One can use the sigmoidal model to predict di-association behavior for both *Vibrio* + *Shewanella* and *Vibrio* + *Aeromonas*, as was done above for the linear model. Again, the predicted neutrophil abundance is consistent with an additive response, but with even larger confidence intervals (Fig. S4K; the sigmoid-model analog of Figure S4E). The available data place only weak constraints on particular functional forms for the neutrophil response. The linear model (linear in log(CFU)) has the virtue of simplicity, with only two relevant parameters, but a deeper understanding of the exact dependence of the immune response on bacterial abundance must await the development of more precise methods.

A simple additive model of bacteria-neutrophil interactions, in which bacteria abundance enhances or suppresses the neutrophil influx rate, is sufficient to explain the neutrophil abundance in di-associations based on parameters largely determined from mono-association experiments. This applies to both the *Vibrio*-*Shewanella* di-association and the *Vibrio*-*Aeromonas* di-association. We note that it is of course conceivable that non-additive interactions among bacteria also exist. It is also certainly possible that

neutrophils can influence bacterial growth rates. With the present data, invoking these and other more complex mechanisms is unwarranted, but these represent fascinating areas of future investigation. It is interesting to notice that this simple model predicts non-monotonic changes in neutrophil abundance over time, due to different effective population “thresholds” for effects on neutrophils by different bacterial species. This may be observable in live imaging experiments, though large numbers of specimens would likely be needed for statistically meaningful outcomes.

The sufficiency of the simple model presented here suggests that understanding bacteria-derived factors that influence neutrophil dynamics may be sufficient to predict their effects on complex, multi-species communities, since impacts on innate immune response may be roughly additive with respect to species.